Differential roles of contrast polarity reveal two streams of second-order visual processing

Isamu Motoyoshi [a,*], Frederick A.A. Kingdom [b]

[a] *Human and Information Science Laboratory, NTT Communication Science Laboratories, NTT 3-1 Morinosato-Wakamiya, Atsugi 243-0198, Japan*
[b] *McGill Vision Research Unit, 687 Pine Avenue West, Rm H4-14, Montreal, Que., Canada H3A 1A1*

Abstract

Humans can easily segregate texture regions based on differences in contrast, orientation, and contrast polarity. It has been suggested that these abilities can be inclusively modeled by 2nd-order visual mechanisms that detect changes in the half-wave rectified outputs of orientation-selective filters. Using a subthreshold-summation paradigm, however, we show that modulations of contrast polarity are detected by mechanisms that pool signals of different orientations while modulations of orientation are detected by mechanisms that pool signals of different contrast polarities. The results support the existence of two streams of 2nd-order processing, one that receives the full-wave rectified inputs from oriented filters, the other separate half-wave rectified outputs from on-center and off-center filters pooled across all orientations. The two-stream model is shown to predict the perceptual effects of changes to the skewness statistics of natural-image textures, and to solve a contradiction among previous data concerning the detection of contrast modulation.
© 2007 Elsevier Ltd. All rights reserved.

Keywords: Pattern; Texture; Luminance; Second-order

1. Introduction

The human visual system is sensitive to changes not only in 1st-order features such as luminance and colour, but also to 2nd-order features such as contrast, orientation and spatial frequency. Psychophysical (Landy & Graham, 2003 for a review) and physiological (Baker, 1999 for a review) evidence supports the idea that 2nd-order mechanisms detect spatial gradients in the nonlinearly transformed responses of 1st-order mechanisms, which can be approximated as a bank of linear filters selective to various orientations and spatial frequencies (Fig. 1a; Bergen & Adelson, 1988; Landy & Bergen, 1991; Graham, Beck, & Sutter, 1992).

Most experimental and computational studies of 2nd-order vision assume that 2nd-order mechanisms detect spatio-temporal changes in the power, but not phase, of the filtered image (see Landy & Graham, 2003). When detect-

ing contrast modulation for example, it is often assumed that the visual system is sensitive to spatial changes in contrast regardless of carrier contrast polarity (Sutter, Sperling, & Chubb, 1995; Langley, Fleet, & Hibbard, 1996; Mareschal & Baker, 1998; Dakin & Mareschal, 2000; Kingdom, Prins, & Hayes, 2003; Motoyoshi & Nishida, 2004). This view may appear reasonable given the definition of a 2nd-order statistic as a measure of image variance, and because the precise position of local image features in textured or stochastic images does not as a rule affect their perceptual properties. However, we are able to discriminate textures solely on the basis of differences in carrier contrast phase (Kingdom, Hayes, & Field, 2001) and can effortlessly segregate textures on the basis of differences in carrier contrast polarity (Rentschler, Hubner, & Caelli, 1988; Malik & Perona, 1990; Hansen & Hess, 2006; Chubb, Econopouly, & Landy, 1994), an illustration of which is shown here in Fig. 1b. We also know that simple cells in V1, which are widely believed to be the neural substrate of 1st-order filters, are selective to contrast

---

* Corresponding author.
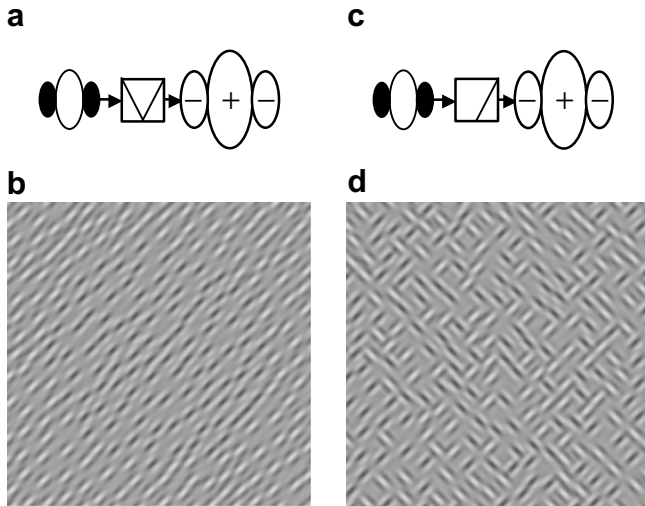*E-mail address:* motoyosi@apollo3.brl.ntt.co.jp (I. Motoyoshi).

Fig. 1. (a) A Filter-Rectify-Filter model of 2nd-order visual processing. The image is first filtered by 1st-order oriented units. 2nd-stage filters then detect spatial changes in the full-wave rectified, or energy, outputs of the 1st-order filters. This model cannot detect the texture region in (b) which is solely defined by the polarity of the elements. A version of the FRF (c) in which the 2nd-stage filters receive half-wave rectified (and thresholded) 1st-order outputs is able to detect the polarity-defined region in (b), but also the region in (d) which is defined by a conjunction of orientation and polarity differences, even though humans cannot segregate it.

phase as well as to orientation and spatial frequency (Hubel & Wiesel, 1968), and that neurons in the retina and LGN can be classified into on-center and off-center units (Schiller, 1982). Taken together these facts suggest that we should expect at least some 2nd-order mechanisms to be sensitive to carrier contrast polarity (from now on referred to simply as polarity).

Second-order mechanisms will be sensitive to carrier polarity if they receive half-wave- rather than full-wave rectified 1st-order filter outputs (Malik & Perona, 1990; see Fig. 1c). However, if those 2nd-order mechanisms are also selective for carrier orientation, as is generally assumed, we should expect the texture in Fig. 1d to effortlessly segregate, yet it does not. The central region of the texture in Fig. 1d consists of right-diagonal bright-center elements and left-diagonal dark-center elements, and the surround region of the complementary pair. No current theory of 2nd-order vision explains why segregation is effortless in Fig. 1b but not in Fig. 1d.

The observations in Fig. 1 may be explained by assuming that the visual system integrates different carrier orientations in polarity-based segregation while integrating different polarities in orientation-based segregation.[1] To test this idea, we measured subthreshold summation between polarity modulations given to differently oriented elements, and between orientation modulations given to different polarity elements. The results show linear summation in both cases. On the basis of these findings we propose a

---

[1] In a brief communication Morrill and Keeble (2001) have reported that the detection of orientation modulation is carrier-polarity unselective.

two-stream model of 2nd-order processing. We also demonstrate that this model correctly predicts the appearance of natural textures with different skewness, or 3rd-order statistics, in different orientation bands, and that it can solve a contradiction in previous data concerning the orientation selectivity of contrast modulation processing.

2. Methods

2.1. Apparatus

Stimuli were generated by a graphics card (CRS ViSaGe) controlled by a host computer (DELL Optiplex GX270), and displayed on a 21-inch CRT (SONY GDM F500R) with a refresh rate of 100 Hz and a luminance resolution of 8 bits. The pixel resolution of the CRT was 1.34 min/pixel at the viewing distance of 1.0 m.

2.2. Stimuli

We used a texture field that subtended 10.7×10.7 deg and contained ∼600 randomly placed elements with a minimum center-to-center separation of 0.31 deg. Half of the elements were bright-center, and half dark-center. At one of four possible quadrants a circular target region with a diameter of 3.58 deg and an eccentricity of 3.13 deg was presented. Portions of the stimuli are shown in Fig. 2.

Each element was the sum of two orthogonally-oriented D2 (oriented-2nd-derivative of Gaussian) luminance profiles (Motoyoshi & Nishida, 2001), i.e.

$$C(x,y) = D2_\theta(x,y) + D2_{\theta+90}(x,y), \tag{1}$$

$$D2_\theta(x,y) = c_\theta \cdot \frac{(x \cdot \cos\theta + y \cdot \sin\theta)^2 - \sigma^2}{\sigma^4} \cdot \exp\left[\frac{-(x^2+y^2)}{2\sigma^2}\right], \tag{2}$$

where σ is the space constant (0.09 deg, i.e., 4 pixels), θ the orientation, and c_θ the luminance contrast. The resulting orientation, contrast, and polarity of each element was manipulated by changing the contrast of the two D2 components ($c_\theta, c_{\theta+90}$). For example, when the contrast of the two D2s was equal, the element was a bright-center or dark-center circular patch traditionally called $\nabla^2 G$ (Marr, 1982), and when the contrasts were different, the element appeared oriented. Thus, we varied the relative contrast of the two orthogonal components of $\nabla^2 G$. The polarity of c_θ and $c_{\theta+90}$ determined whether the element was bright-center or dark-center. The space-averaged luminance of each D2 patch had a Michelson contrast of only 0.00007 ($\Delta L = 0.0028$ cd/m^2) with respect to the uniform background of 40 cd/m^2. It was thus impossible to segregate the target region based on mean luminance, i.e., 1st-order properties.

The absolute orientation of the D2 pattern (θ) was randomized on every stimulus presentation to minimize local orientation adaptation and minimize the possibility of subjects using specific features to perform the task (e.g., searching for vertically oriented elements or regions).

Polarity modulation. Polarity modulations were obtained by modulating the contrasts of the bright-center and dark-center elements out of phase between target and background (Fig. 2a). To test for summation across orientations, the modulations were independently given to two orthogonal orientations, θ and $\theta+90$:

$$\begin{aligned}
c_{B,\theta} &= C_{mean} \cdot (1 + k \cdot M_\theta) \\
c_{B,\theta+90} &= C_{mean} \cdot (1 - k \cdot M_{\theta+90}) \\
c_{D,\theta} &= -C_{mean} \cdot (1 - k \cdot M_\theta), \\
c_{D,\theta+90} &= -C_{mean} \cdot (1 + k \cdot M_{\theta+90})
\end{aligned} \tag{3}$$

where C_{mean} (=0.25) is the mean contrast of the D2 component, M the modulation depth and κ the polarity of contrast modulation, which was always 1.0 for elements in the target region and −1.0 in the background region (note κ is NOT the polarity of the elements).
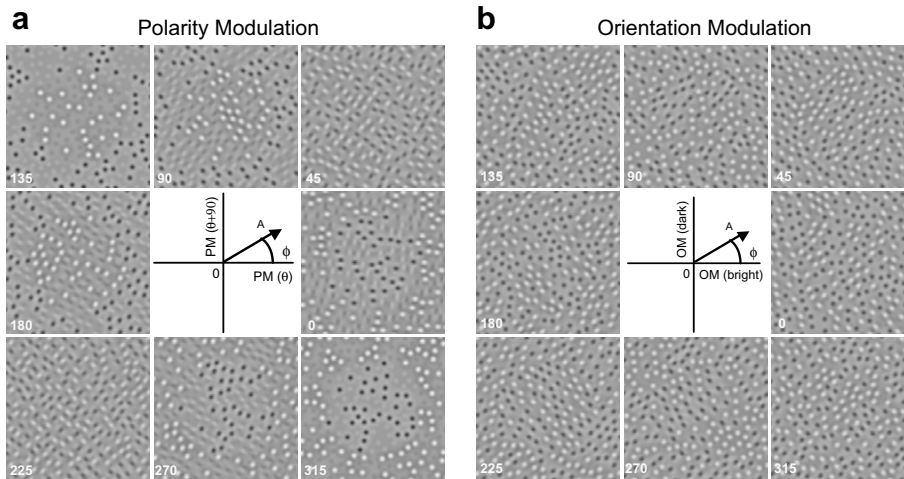
Fig. 2. Portions of stimuli used in experiments. (a) Polarity modulated stimuli. The relative contrast strength of the bright-centre and dark-centre elements was independently varied for different orientations between the target and background in accordance with a vector of length *A* and direction *ϕ*. (b) Orientation modulated stimuli. The relative orientation strength of the bright- and dark-centre elements was independently varied between the target and background.

Orientation modulation. Orientation modulations were obtained by changing the strength of orientation in the elements out of phase between target and background (Fig. 2b). The orientation "strength" was controlled by the relative contrast of the two orthogonal D2 components as described above (the elements were circular when the contrasts were the same). To test for summation across polarities, the modulations were given separately to the bright-center and dark-center elements:

$$c_{B,\theta} = C_{mean} \cdot (1 + \kappa \cdot M_B)$$
$$c_{B,\theta+90} = C_{mean} \cdot (1 - \kappa \cdot M_B)$$
$$c_{D,\theta} = -C_{mean} \cdot (1 + \kappa \cdot M_D) \quad (4)$$
$$c_{D,\theta+90} = -C_{mean} \cdot (1 - \kappa \cdot M_D)$$

For both polarity and orientation modulations, the depths of the two separate modulations (M_θ and $M_{\theta+9}$ for polarity modulation; M_B and M_D for orientation modulation) were controlled by the vector with strength of *A* and direction *ϕ* as illustrated in the central panel of Fig. 2a and b.

2.3. Procedure

We measured modulation thresholds for detecting the target region using a spatial 4AFC procedure. On each trial, the target region was presented in one of the four quadrants for 300 ms. Subjects viewed the stimuli binocularly while fixating a black dot at the center of the display, and indicated the location of the target region by pressing one of four buttons. An incorrect response was followed by a tone. The next trial started about 0.5 s after the subject's response.

Thresholds were estimated by a staircase method. Within each staircase, the vector length (*A* in the central panel of Fig. 2a and b) that controlled the modulation amplitude of the two component texture modulations was decreased by 0.05 log unit after two correct responses, and increased by the same amount after one incorrect response. In order to minimize the possibility that subjects used specific features to perform the task, such as searching for bright blobs, the staircases for the different vector directions (*ϕ* in the central panel of Fig. 2a and b) were randomly interleaved within a single measurement session. In each session, the staircase terminated when the number of trials in one of the staircases exceeded 30, and the session was repeated until the total number of trials for each condition exceeded ∼200. The final threshold estimates, which gave 62.5% correct and their 95% confidence intervals were calculated, respectively, by means of a maximum likelihood method and bootstrapping (400 samples).

2.4. Subjects

Three naïve (A.M., J.M., K.K.) and one author (I.M.) served as subjects. All had corrected-to-normal vision. K.K. participated only in the polarity modulation Experiment, and J.M. only in the orientation modulation experiment.

3. Results

Fig. 3a shows thresholds for the polarity modulation experiment in terms of the polarity-modulation depths given to the elements with one orientation (M_θ; *x*-axis) and the other orientation ($M_{\theta+90}$; *y*-axis). Fig. 3b shows thresholds for the orientation modulation experiment in terms of the orientation-modulation depths of the bright-center (M_B; *x*-axis) and dark-center (M_D; *y*-axis) elements. For both experiments, thresholds are on, or very close to the diagonal straight line, indicating linear summation between modulations of different carrier properties. These results show that visual mechanisms responsible for detecting polarity modulations integrate across different carrier orientations while those responsible for detecting orientation modulations integrate across different polarities.

4. Discussion

As mentioned earlier, previous studies (Rentschler et al., 1988; Malik & Perona, 1990; Hansen & Hess, 2006; Chubb et al., 1994) have demonstrated texture segregation based on differences in contrast polarity (see Fig. 1b) and proposed 2nd-order visual mechanisms that receive polarity-specific inputs from orientation-selective filters such as simple cells (Fig. 1c). However, our demonstration in Fig. 1d, together with the subthreshold-summation data, reveal that the human visual system does not have
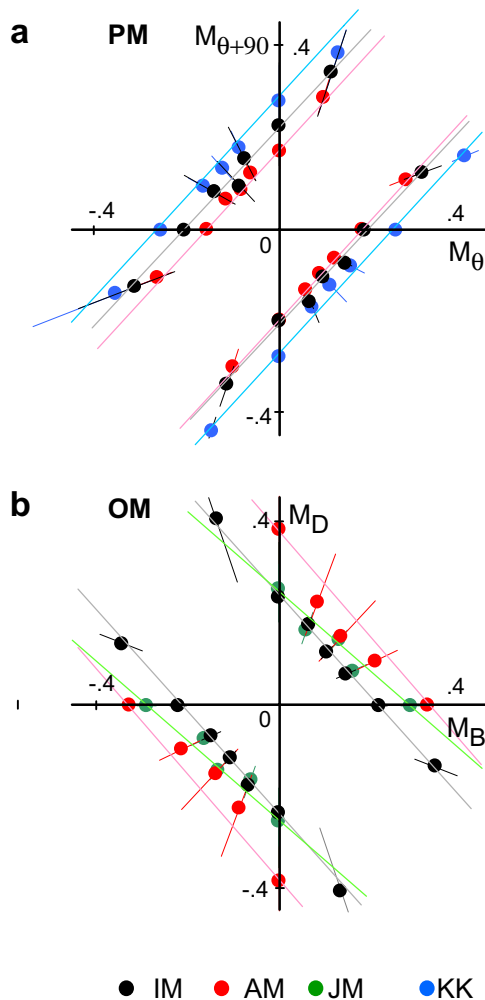
Fig. 3. (a) The results for polarity modulation. The data are plotted as a function of the modulation depth of one (M_θ) and the other ($M_{\theta+90}$) orientation. (b) The results for orientation modulation. The data are plotted as a function of the modulation depth of the bright-centre (M_B) and the dark-centre elements (M_D). Different colors represent different observers. Error bars represent 95% confidence intervals. Solid lines are the predictions of linear summation.

2nd-order mechanisms that are selective to both carrier orientation and carrier polarity.

As the simplest interpretation of this finding, we propose that there exist at least two streams of 2nd-order processing. One stream analyzes the spatial distribution of orientation information regardless of polarity, the other the spatial distribution of polarity information regardless of orientation.

4.1. Two-stream model

The two-streams can be modeled as shown in Fig. 4a, by the least modification of the standard FRF model shown in Fig. 1a and c. The model posits two streams of 2nd-order processing, the "orientation" (red) and "phase" (green) streams. The orientation stream takes as input the full-wave rectified outputs of Gabor-like 1st-order filters

selective to orientation, and hence is sensitive to carrier orientation but not polarity, as with complex cells in V1 (Hubel & Wiesel, 1968). The phase stream on the other hand takes as input the half-wave rectified outputs of on- and off-center isotropic filters, and hence is sensitive to carrier polarity but not orientation, as with LGN cells or V1 blob cells (e.g., Schiller, 1982; Livingstone & Hubel, 1984). Fig. 4b shows a version of the model that is functionally equivalent to that shown in Fig. 4a. In Fig. 4b, the phase mechanism (green) linearly integrates the half-wave rectified outputs of Gabor-like filters across orientation. Note that both model versions are subject to more complex non-linearities than rectification (implied by "NL" in the figure), including gain-control and cross-orientation interactions (e.g., Heeger, 1991; Motoyoshi & Kingdom, 2003). In both model versions, spatial modulations in orientation and polarity are detectable only by the orientation and phase streams, respectively. For orientation modulations, only the orientation stream will be responsive because the phase stream is insensitive to carrier orientation, while for polarity modulations only the phase stream will be responsive because the orientation stream is insensitive to carrier polarity.

Both versions of the model in Fig. 4 assume that the 1st-stage inputs into the phase stream are half-wave rectified, and in the version in Fig. 4b, also the 1st-stage inputs to the orientation stream. How valid is the assumption of half-wave-rectification? It is theoretically possible that a single, linear, signed-polarity channel could be the input to the phase stream,[2] and from a strict engineering point of view, this would be more parsimonious than dual half-wave rectified inputs (Chubb, Landy, & Econopouly, 2004). However, evidence suggests that local increments and decrements are processed by separate mechanisms at an early stage in vision. For example, we are unable to dichoptically fuse increments with decrements, even though two different-in-contrast increments, or two different-in-contrast decrements, can be fused (Whittle, 1965; Kingdom, 2003). Moreover, increments fail to mask, or adapt the detection of decrements, and vice-versa, even though increments mask/adapt increments and decrements mask/adapt decrements (Sankeralli & Mullen, 2001; Purkiss, Hughes, & Demarco, 2001). Neither result is consistent with a single bipolar mechanism for detecting increments and decrements. Added to this is the physiological evidence for separate "On" and "Off" channels at the earliest stages of vision (Schiller, 1982). Thus we argue that given the available evidence, half-wave rectified 1st-stage inputs to both the phase and orientation streams is the most likely scenario.

We assume that inputs to both streams are also selective to spatial frequency. This assumption is based on the fact that almost all front-end units in the early visual system are selective to spatial frequency though not always

---

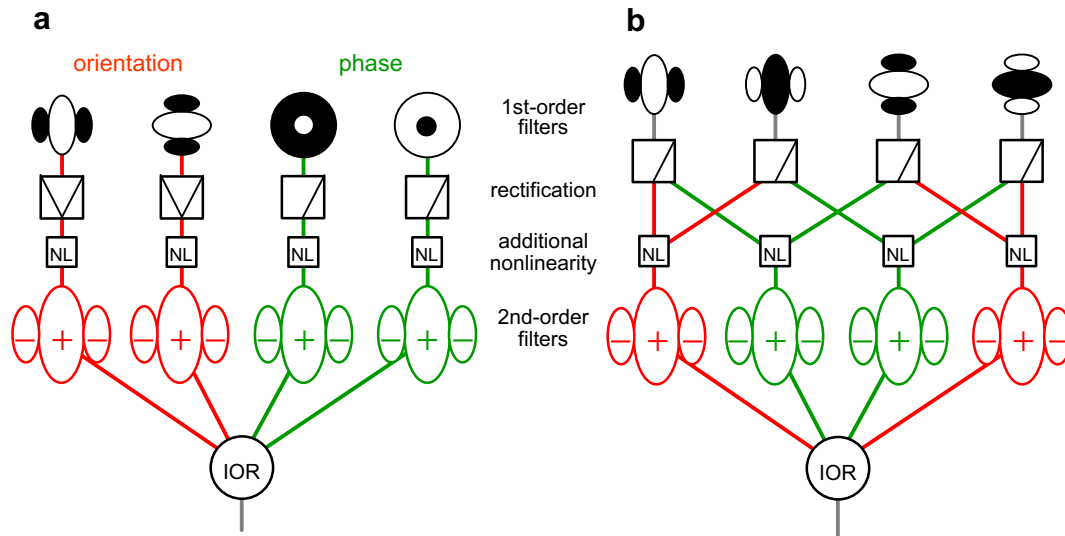[2] We are grateful to Charlie Chubb for pointing out to us this possibility.

Fig. 4. Schematic diagram of FRF models that are consistent with the results. The two models in (a) and (b) both assume two types of 2nd-order mechanism. The "orientation" mechanism denoted by red receives the full-wave rectified outputs from Gabor-like 1st-order filters, and is selective to their orientation, but not phase. The "phase" mechanism denoted by green receives the half-wave rectified outputs of (a) isotropic filters of a particular phase, or (b) oriented filters summed across orientation, of a particular phase. The outputs of all 2nd-order mechanisms are probabilistically (or RMS) summed. Note that the two versions of the model are functionally almost equivalent.

narrowly tuned. Moreover, as demonstrated in Fig. 5, texture regions defined by a conjunction of polarity and spatial frequency can be effortlessly segregated, contrary to what is found with the polarity-orientation conjunction shown in Fig. 1d. This seems to suggest that polarity-sensitive 2nd-order mechanisms (the phase stream in Fig. 4) are also sensitive to spatial frequency. A demonstration with natural textures described below also supports this idea, but further experiments will be necessary to provide a robust confirmation.

4.2. A test with natural images

Recent psychophysical and computer-vision studies have posed the question of what image statistics (variance, skew, kurtosis, coherency, etc.) are used by the visual system to discriminate natural textures. Those statistics might
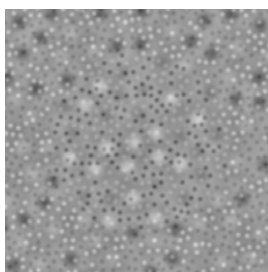

Fig. 5. A texture region defined by a conjunction of the polarity and the size (spatial frequency) of elements. The central region consists of large bright elements and small dark elements while the background of large dark elements and small bright elements. In contrast to the analogous case of polarity-orientation conjunction in Fig. 1d, human can effortlessly segregate this texture.

be called "texture metrics". Heeger and Bergen (1995) demonstrated that equalizing the luminance and sub-band (orientation × SF) histograms of white noise to those of a natural texture produces a synthetic texture that is perceptually similar, and sometimes even identical, to the original texture (see also Portilla & Simoncelli, 2000). More recently, Kingdom et al. (2001) measured sensitivity to differences in the lower-order moments of the wavelet histograms of stochastic $1/f$ textures, and found unexpectedly high sensitivities to differences in kurtosis, or the 4th-order moment. All computational models of texture vision make predictions as to which texture metrics the visual system is sensitive. For example, the standard FRF model (Landy & Graham, 2003) encodes variance and carries information about kurtosis (though to produce a signal that corresponds to the spatio-temporal pattern of kurtosis the model requires an additional stage of rectification and filtering—see Kingdom et al., 2001) but carries no information about skewness because of the full-wave rectification of the 1st-order outputs. On the other hand, the Malik and Perona (1990) type FRF model can encode skewness because it half-wave rectifies its inputs.

The model(s) in Fig. 4 can encode variance and carry information about kurtosis as with the standard FRF. It can also encode skewness, as in Malik and Perona's (1990) model, but not within each sub-band. This is because the phase-sensitive mechanisms that encode skewness, while sensitive to carrier spatial frequency, are not sensitive to carrier orientation, as we have demonstrated empirically. Thus, our psychophysical data and the model(s) in Fig. 4 predicts that the visual system will be sensitive to skewness within a spatial-frequency sub-band, but not within an orientation sub-band.

To test this prediction we have skewed the histogram of a natural texture image (taken from the foliage section of Olmos & Kingdom, 2004) within either a spatial frequency or an orientation sub-band, and the results are shown in Fig. 6 (see Appendix A for the method). In Fig. 6a the sub-band histogram of a 1 octave range of spatial frequencies centred on 16 c/image has been skewed in opposite directions, while in Fig. 6b the same skewing operation has been applied to a 30 deg range of orientations centred on vertical. It is clear that the perceptual effects of differential skewing are much more profound in (a) than in (b). Similar results are obtained for a different natural texture ((c) and (e); coffee beans, MIT VisTex Database), and for $1/f^{0.5}$ noise ((d) and (f)), for which there are no correlations across spatial frequency or orientation, ruling out the possibility that the effect is an artifact of the higher-order structure of natural images. It should be noted however that if the images are scrutinized (Rentschler et al., 1988), it is not hard to discriminate the pairs in which orientation-subband histogram skewing has been applied ((b), (e), and (f)). This kind of analysis-by-synthesis approach

might be employed to reveal whether sensitivity to other lower-order moments, such as kurtosis, is tuned to orientation and spatial frequency, and also the extent to which the human visual system is sensitive to higher-order image statistics (e.g., the 5th-order moment).

4.3. Implications for contrast modulation processing

The model(s) in Fig. 4 will also respond to modulations of other 2nd-order features, such as contrast. Contrast modulations would be detectable because the 1st-order inputs from both streams are sensitive to carrier contrast. Thus potentially the two-stream model has general applicability. However the data provided above in no sense proves that contrast modulations are detected by the two-stream model. Nevertheless, we have found that the model(s) can reconcile a contradiction in previous data concerning the carrier orientation tuning properties of contrast modulation detection. This constitutes one piece of evidence in favor of the idea that the two-stream model also mediates the detection of contrast modulation.
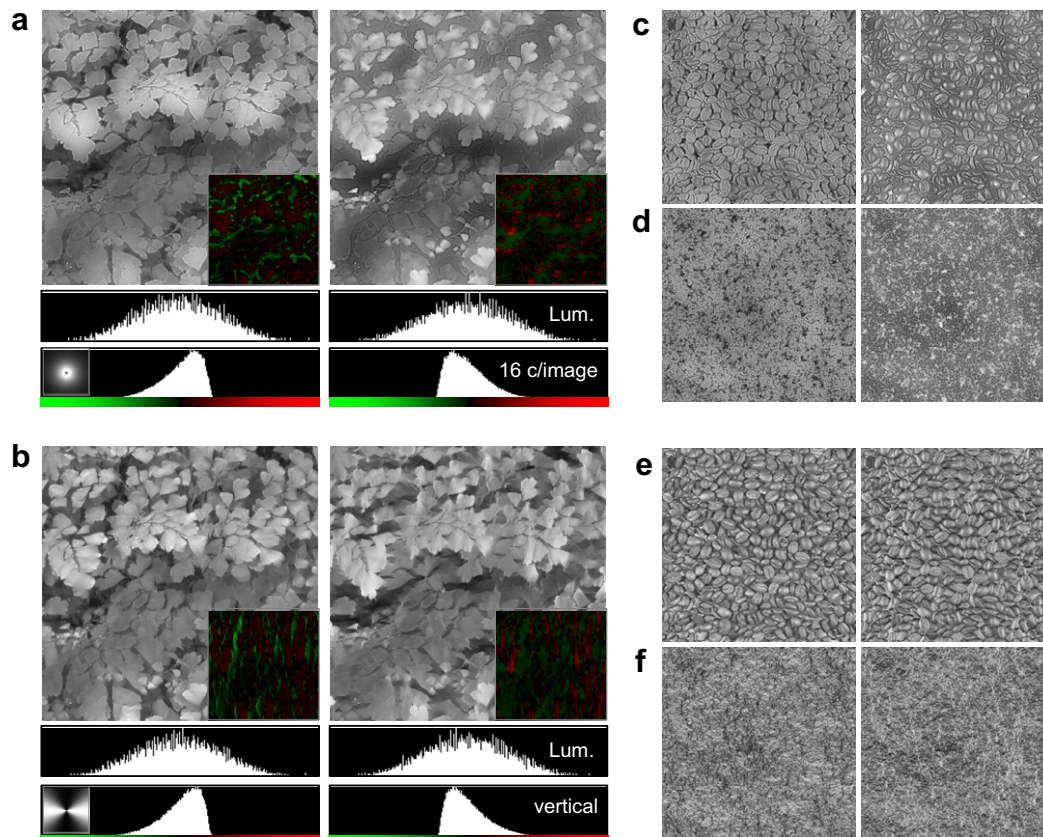

Fig. 6. A demonstration of how skewness in the wavelet histogram at a particular spatial-frequency band (a, c, and d) and at a particular orientation band (b, e, and f) affects the discriminability of natural textures. (a) The upper two images are natural textures in which the sub-band histograms within a 1.5 octave bandwidth centred on 16 c/image were matched to Beta functions skewed negatively (left) and positively (right), while maintaining the pixel histogram at zero skew (to achieve this the other bands are each skewed by a small amount in the opposite direction). Insets are the sub-band images representing the on- (red) and off- (green) 1st-order filters responses. The luminance and wavelet histograms are shown below the image. An inset of the sub-band histogram represents the spectrum of the band-pass filter employed. (b) The same method applied to the orientation domain. This time the skewed sub-band is a 30 deg orientation bandwidth centred on vertical. (c–f) Resulting images of two textures whose sub-band histograms are skewed negatively (left) and positively (right). Note that the perceptual effect of skewness is more profound in (a, c, and d) than in (b, e, and f). See text for further details.

a

● IM   ● SN   ● YT   ● CH

b

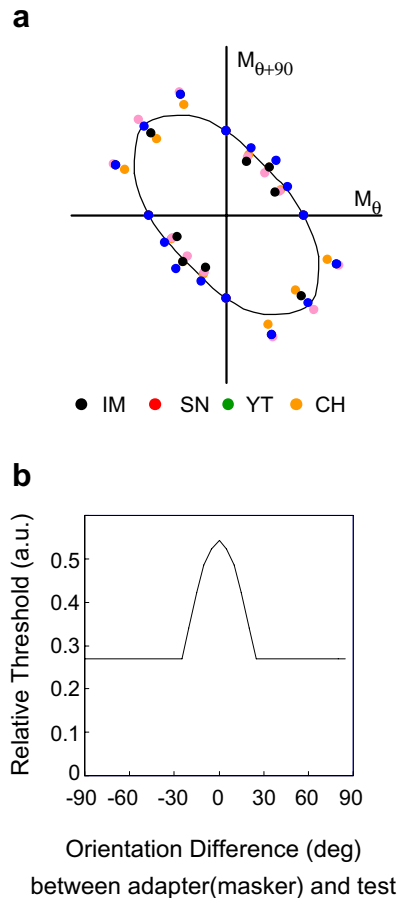Orientation Difference (deg)

between adapter(masker) and test

Fig. 7. Simulation of previous psychophysical findings by the model in Fig. 4. (a) Quasi-linear summation between two contrast modulations with orthogonal carrier orientations. The circles represent the normalized thresholds from Motoyoshi and Nishida (2004), plotted as a function of the depth of contrast modulation at one orientation (M_θ) and the orthogonal orientation ($M_{\theta+90}$). The solid line represents the predicted thresholds. (b) The modeled effect of an unmodulated adaptor/mask of variable carrier orientation on the detection of contrast modulation of fixed carrier orientation, predicting the results of Dakin and Mareschal (2000).

Langley et al. (1996) and Dakin and Mareschal (2000) have demonstrated that thresholds for detecting contrast modulations are selectively elevated by adaptation to, or masking by unmodulated stimuli with a similar carrier orientation. This has been interpreted as evidence that contrast modulations are processed by mechanisms selective to carrier orientation (Langley et al., 1996; Dakin & Mareschal, 2000). On the other hand, Motoyoshi and Nishida (2004) found quasi-linear summation between contrast modulations with orthogonal carriers, suggesting that contrast modulations are processed by mechanisms unselective to carrier orientation. These apparently contradictory findings are resolved by the model(s) in Fig. 4, where contrast modulations can be detected by both orientation-selective (orientation stream) and non-selective (phase stream) mechanisms. Fig. 7a shows the predicted (solid line) and observed (circles) thresholds for the stimuli of Motoyoshi

and Nishida (2004).[3] The predicted thresholds are simply calculated as the (normalized) inverse of the output of the model in Fig. 4b without any additional nonlinear stage. Although some data deviate from the prediction, the model successfully captures the quasi-linear summation between contrast modulations of orthogonal carrier orientations. Fig. 7b shows the predicted thresholds for contrast modulations when the contrast inputs to the model were reduced within a particular orientation range (Gaussian of 30 deg bandwidth) due either to adaptation (Langley et al., 1996) or masking (Dakin & Mareschal, 2000). The model qualitatively predicts the orientation-selective threshold elevations.

Appendix A. Sub-band histogram manipulation

The sub-band skewed images in Fig. 6 were constructed by an iterative processes similar to that employed by Motoyoshi, Nishida, Sharan, and Adelson (2007). (1) The luminance image was filtered by a Gaussian isotropic filter with a peak frequency of 8 c/image and a bandwidth of 1.0 octave (Fig. 6a), or by a Gaussian orientation-wedge filter peaking at 0 deg with a bandwidth of 25 deg (Fig. 6b). (2) The histogram of the band-pass filtered image was matched to a Beta distribution with a skewness of 0.9 or −0.9, while the SD (standard deviation) was kept the same at a value of 0.3. The Beta distribution was given as follows:

$$f(l) = \frac{1}{B(p,q)} l^{p-1}(1-l)^{q-1},$$

$$B(p,q) = \int_0^1 l^{p-1}(1-l)^{q-1}\,dl, \tag{A1}$$

where l is luminance, p and q are parameters related to the amount of skew ($p = 1.5/q = 8.5$, or $p = 8.5/q = 1.5$). The mean and SD were controlled by rescaling the Beta distribution. (3) The modified filtered image was integrated with the residual, band-cut image. (4) the histogram of the integrated image was matched to a Beta distribution with skewness ($p = 5/q = 5$) of zero. Eight iterations were employed.

---

[3] Motoyoshi and Nishida (2004) found significantly higher thresholds for the detection of decremental compared to incremental contrast targets. The data plotted in Fig. 6a are the average of the two conditions.

References

Baker, C. L., Jr. (1999). Central neural mechanisms for detecting second-order motion. *Current Opinion in Neurobiology, 9*, 461–466.

Bergen, J. R., & Adelson, E. H. (1988). Early vision and texture perception. *Nature, 333*, 363–364.

Chubb, C., Econopouly, J., & Landy, M. S. (1994). Histogram contrast analysis and the visual segregation of IID textures. *Journal of the Optical Society of America A, 11*, 2350–2374.

Chubb, C., Landy, M. S., & Econopouly, J. (2004). A visual mechanism tuned to black. *Vision Research, 44*, 3223–3232.

Dakin, S. C., & Mareschal, I. (2000). Sensitivity to contrast modulation depends on carrier spatial frequency and orientation. *Vision Research, 40*, 311–329.

Graham, N., Beck, J., & Sutter, A. (1992). Nonlinear processes in spatial-frequency channel models of perceived segregation: effects of sign and amount of contrast. *Vision Research, 32*, 719–743.

Hansen, B. C., & Hess, R. F. (2006). The role of spatial phase in texture segmentation and contour integration. *Journal of Vision, 6*, 594–615.

Heeger, D. J. (1991). Nonlinear model of neural responses in cat visual cortex. In M. S. Landy & A. J. Movshon (Eds.), *Computational models of visual processing* (pp. 119–133). Cambridge, Massachusetts: The MIT Press.

Heeger, D. J., & Bergen, J. R. (1995). Pyramid-based texture analysis/synthesis. *Computer graphics proceedings*, 229–238.

Hubel, D. H., & Wiesel, T. N. (1968). Receptive fields and functional architecture of monkey striate cortex. *Journal of Physiology (London), 195*, 215–243.

Kingdom, F. A. A. (2003). Levels of Brightness Perception. In L. Harris & M. Jenkin (Eds.), *Levels of perception*. Springer–Verlag.

Kingdom, F. A. A., Hayes, A., & Field, D. J. (2001). Sensitivity to contrast histogram differences in synthetic wavelet-textures. *Vision Research, 41*, 585–598.

Kingdom, F. A. A., Prins, N., & Hayes, A. (2003). Mechanism independence for texture-modulation detection is consistent with a Filter-Rectify-Filter mechanism. *Visual Neuroscience, 20*, 65–76.

Landy, M. S., & Bergen, J. R. (1991). Texture segregation and orientation gradient. *Vision Research, 31*, 679–691.

Landy, M., & Graham, N. (2003). Visual perception of texture. In L. M. Chalupa & J. S. Werner (Eds.). *The visual neurosciences* (Vol. 2, pp. 1106–1118). MIT press.

Langley, K., Fleet, D. J., & Hibbard, P. B. (1996). Linear filtering precedes nonlinear processing in early vision. *Current Biology, 6*, 891–896.

Livingstone, M. S., & Hubel, D. H. (1984). Anatomy and physiology of a color system in the primate visual cortex. *Journal of Neuroscience, 4*, 309–356.

Malik, J., & Perona, P. (1990). Peattentive texture discrimination with early vision mechanisms. *Journal of the Optical Society of America A, 7*, 923–932.

Mareschal, I., & Baker, C. L. Jr., (1998). A cortical locus for the processing of contrast-defined contours. *Nature Neuroscience, 1*, 150–154.

Marr, D. (1982). *Vision: a computational investigation into the human representation and processing of visual information*. New York: WH Freeman and Company.

Morrill, P., & Keeble, D. R. T. (2001). Can polarity be ignored in the visual processing of micropattern orientation and texture segmentation? *Perception, 30*(Suppl.), 92.

Motoyoshi, I., & Kingdom, F. A. A. (2003). Energy–frequency analysis reveals orientation-opponent channels in human vision. *Vision Research, 43*, 2197–2205.

Motoyoshi, I., & Nishida, S. (2001). Temporal-resolution of orientation-based texture segregation. *Vision Research, 41*, 2089–2105.

Motoyoshi, I., & Nishida, S. (2004). Cross-orientation summation in texture segregation. *Vision Research, 44*, 2567–2576.

Motoyoshi, I., Nishida, S., Sharan, L., & Adelson, E. H. (2007). Image statistics and the perception of surface qualities. *Nature, 447*, 206–209.

Olmos, A., & Kingdom, F. A. A. (2004). McGill Calibrated Colour Image Database. Available from http://tabby.vision.mcgill.ca.

Portilla, J., & Simoncelli, E. P. (2000). A parametric texture model based on joint statistics of complex wavelet coefficients. *International Journal of Computer Vision, 40*, 49–71.

Purkiss, T. J., Hughes, A., & Demarco, P. J. Jr., (2001). Processing of scotopic increments and decrements. *Visual Neuroscience, 18*, 119–125.

Rentschler, I., Hubner, M., & Caelli, T. (1988). On the discrimination of compound Gabor signals and textures. *Vision Research, 28*, 279–291.

Sankeralli, M. J., & Mullen, K. T. (2001). Bipolar or rectified chromatic detection mechanisms. *Visual Neuroscience, 18*, 127–135.

Schiller, P. H. (1982). Central connections of the retinal ON and OFF pathways. *Nature, 297*, 580–583.

Sutter, A., Sperling, G., & Chubb, C. (1995). Measuring the spatial frequency selectivity of second-order texture mechanisms. *Vision Research, 35*, 915–924.

Whittle, P. (1965). Binocular rivalry and the contrast at contours. *Quarterly Journal of Experimental Psychology, 17*, 217–226.